



Green Synthesis of Silver Nanoparticles Using *Nymphae odorata* Extract Incorporated Films and Antimicrobial Activity

Apparao Gudimalla^{1,2,3} · Jiya Jose² · Rajendran Jose Varghese² · Sabu Thomas²

Accepted: 29 October 2020 / Published online: 15 November 2020
© Springer Science+Business Media, LLC, part of Springer Nature 2020

Abstract

Silver nanoparticles (AgNPs) synthesis was formulated by the green method using *Nymphae odorata* plant extract as reducing and capping agent. Plants offer a good platform for synthesizing nanoparticles (NPs) which can act as a non-toxic, natural capping/reducing agent and can convert Ag^+ to Ag^0 . The 5 min reduction time (the extract contains a lot of reduction agents, which leads to quick synthesis and such can be a great advantage) is a best experimental condition for the effective biological synthesis of AgNPs. Sodium alginate films were doped by these NPs. The antimicrobial study of AgNPs and doped films were examined by *Staphylococcus aureus* and *Escherichia coli*. As a result, at very low concentration of about 25 μl of AgNPs was found to inhibit the entire bacterial strains studied and films also showed a similar result. The results confirmed the effectiveness of prepared AgNPs and films as an antibacterial agent. Hence, it can be used for nano-biotechnology, biomedical and industrial applications.

Keywords Green synthesis · Nanoparticles · Sodium alginate · Films · Antimicrobial activity

Introduction

In recent years, nanotechnology has been widely used in a huge range of applications and several new disciplines in many areas. It deals with visualization, manipulation, and fabrication of materials at the nanoscale level [1]. In such a way, the Silver nanoparticles (AgNPs) have gained extensive awareness in the field of medicine, biotechnology, pharmacology, food packaging and energy storage [2]. Nano-biotechnology is a rapidly growing field as integration between biotechnology and nanotechnology for developing biosynthetic and eco-friendly technology to manufacture new materials at the nanoscale level [3]. The unique properties of nanomaterials have attracted significant attention for their pharmaceutical applications. Especially, in the field

of nano-medicine can play a significant role in developing alternative and more effective treatment strategies for the treatment of many diseases [4].

The fabrication of nanoparticles (NPs) conducts into two types of approaches such as top-down and bottom-up. NP synthesis usually uses laser ablation, pyrolysis, sol-gel, vapour deposition and electrodeposition. Various chemical and physical strategies are being used for NPs production. However, most of the techniques adopted expensive methods using toxic chemicals, stabilizing and capping agents [5]. To overcome these problems, the environmentally friendly green synthesis method was developed [6]. Plants offer a good platform for synthesizing NPs and acts as a non-toxic, natural capping/reducing agent [7, 8]. This green synthesis offers a single-step method which has several advantages such as efficient and relevant method, cost-effective and very easy process compared to other methods [9–12]. The reduction and stabilizing of metal ions with plant extract is reported to be higher than microorganisms and other biosynthetic methodology [13]. The plant extract contains various biomolecules with hydroxyl group and the carboxylic groups and can act as stabilizers and reducing agents. Not only plant leaf, but other plant parts like fruit, bark, fruit peels, roots, and callus have also been used for the synthesis of metal NPs such as Ag, Au, Pt etc. in several sizes and shapes [14].

✉ Apparao Gudimalla
appigspl@gmail.com; appigspl@yahoo.in

¹ Department of Nanotechnology, Acharya Nagarjuna University, Nagarjuna Nagar 522 510, A.P., India

² International and Inter University Center for Nanoscience and Nanotechnology, Mahatma Gandhi University, Kottayam, Kerala 686560, India

³ Jožef Stefan International Postgraduate School, Jamova cesta 39, 1000 Ljubljana, Slovenia

The progress of a green process for the AgNPs synthesis is a trend of modern nano-biotechnology study [14]. It's well-known that the silver has been used for a long time for the effective antibacterial activity [15]. Among the AgNPs synthesized from the plant extracts have been studied for their different properties from biology such as anthelmintic [16], antilarvicidal [17], antioxidant, anticancer, wound healing [18, 19], hepatoprotective and antimicrobial activity [20, 21]. The antimicrobial activity of AgNPs permits them to be correctly used in various household products like home appliances, food containers for storage and textiles.

The foremost necessary use of AgNPs and silver into the medicinal product like tropical ointments for the treatment of open wounds and burns [22, 23]. This work explored the use of *Nymphae odorata* plant extract to prepare AgNPs. As synthesized AgNPs were incorporated into sodium alginate film, these composite films were tested for its antimicrobial property. Several studies were reported that natural biopolymers such as alginate, cellulose, agar, starch, gelatin, etc. have been used as a capping and reducing agent for NPs production [24, 25]. Nevertheless, synthesis of metallic NPs has been attracted significant interest due to their unique properties.

Alginate is a naturally derived polymer and has a great interest in the different areas of nanomedicine from several decades [26, 27]. It has extensive properties such as renewability, biocompatibility, biodegradability, less toxicity and is capable of easy surface modification. Moreover, the similarity of these materials to human tissues made these materials to apply in wound healing and also in food packaging [28, 29]. It is a natural polymer composed of (1→4)—linked β -D-mannuronic (M) and α -L-guluronic (G) residues in various covalent blocks are a perfect substance for the treatment of wound healing [30–32]. Generally, the acid monomers divided by two homo-polymeric blocks with a similar alternating order [33]. Alginate is water-soluble [34] and it

could able to be cross-linked by Zn^{2+} , Ca^{2+} , Ba^{2+} and Cu^{2+} [35]. Alginate films are hydrophilic and easily dissolved in water and have low mechanical properties. With the help of cross-linking the hydrophilic nature can be reduced and mechanical properties can be increased [36]. AgNPs incorporated alginate films have been mostly used for magnetic, catalytic, optical, thermal, electrical permanence, antibacterial activity [37], biomedical applications (cartilage, bone, soft tissue regeneration) [38, 39], controlled-release delivery system [40], wound dressing [41] and in membrane applications [42]. Recently, the wound dressing is active development, with intend of imparting particular functions [43]. The present work is to formulate a wound dressing material by enhancing the property using phytochemicals.

In this report, we prepared AgNPs using *Nymphae odorata* leaves through the development of a novel, facile and green method. And these silver nanoparticles were incorporated into sodium alginate films. The prepared composites could be employed as drug delivery, wound dressing, antimicrobial protection, biological sensor and food packing materials.

Experimental Section

Materials Used

Nymphae odorata (Waterlily) leaves shown in Fig. 1 were collected from Kottayam, Kerala, India. AgNO_3 , ZnCl_2 , Sodium Alginate, Glycerol, Nutrient broth and Agar-agar were purchased from Sigma-Aldrich.

Preparation of Plant Extract

The *Nymphae odorata* extract was used based on cost effective, eco-friendly and ease availability/processing. The plant

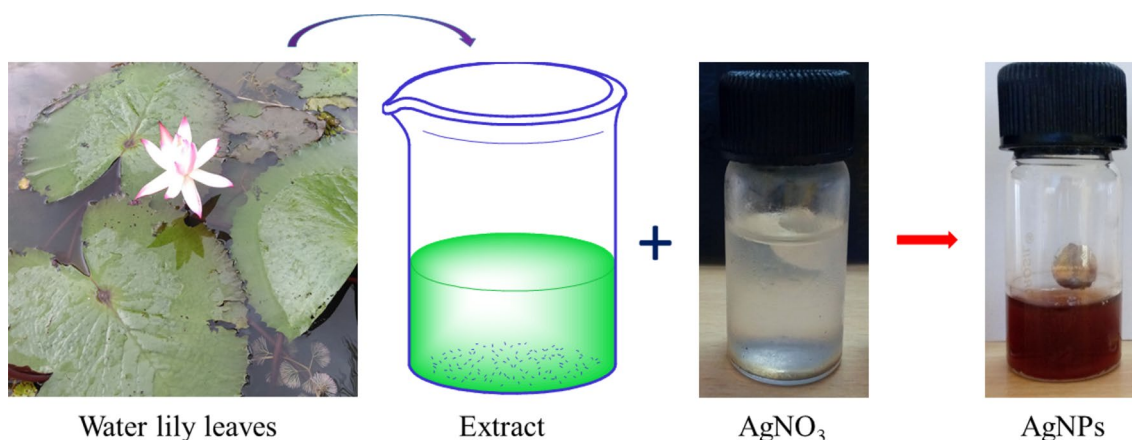


Fig. 1 Synthesis of silver nanoparticles by using plant extract

leaves were washed with deionized (DI) water to get rid of impurities and cut into fine pieces. Then the leaves were dried in a hot air oven at 90 °C for 2 h. After that, the dried leaves were powdered and 1 g of powdered was added to 50 mL of DI water and then the system was boiled with water bath at 95 °C for 2 h. Finally, the stewed solution was filtered through Whatman No. 1 paper and the filtered solution was stored in the refrigerator for further experiments.

Synthesis of AgNPs

For the synthesis, the prepared plant extract was used as a reducing/stabilizing agent for the process of bioreduction. 1 mM aqueous AgNO₃ solution was prepared in an Erlenmeyer flask and 10 mL of the prepared 1 mM AgNO₃ solution was added with 1 mL (10:1 ratio) of plant extract. Then the mixed solution was kept in a water bath at 95 °C for 5 min (Fig. 1). The reduction of Ag⁺ to Ag⁰ was confirmed by the colour change from pale light to yellow, finally, it was settled as a reddish-brown colour solution. This bioreduction was due to the plant extract which acts as both stabilizing and reducing agent and this leads to the formation of AgNPs. It is well acknowledged that AgNPs showed yellowish-brown colour due to excitation of SPR (surface plasmon resonance) in AgNPs, and this was confirmed by UV spectroscopy.

Preparation of AgNPs Loaded Films

Solvent casting method was used for the preparation of AgNPs incorporated sodium alginate (SA) composite films (Fig. 2). For preparing SA composite film, 2 wt% of SA powder was dispersed in DI water and then stirred with the magnetic stirrer at 70 °C/30 min. Next, a few drops of glycerol were added to the solution and stirred for 10 min. Glycerol was used as a plasticizer to avoid the premature breaking of the film. Thereafter, the well-dispersed solution was used to cast the film layered on a glass plate, then casted film was dried at room temperature for 24 h, after that the film was placed in the oven at 45 °C/10 min. Finally, 5% of the ZnCl₂ solution was added to the dried film for cross-linking (1 h), to eliminate the traces of ZnCl₂ solution and the film was washed with DI water. Similarly, AgNPs incorporated films were prepared by mixing an equal amount (1:1) of SA and AgNPs solution and cast. The prepared films have a smooth surface with average thickness as you can observe in Table 1 and it does not have bends or breaks as you see them in Fig. 3.

Table 1 The composite film's thickness and water sensitivity test values

Samples	Thickness (mm)	Moisture (%)	Solubility (%)	Absorption (%)
ALG	0.174 ± 0.008	46.50 ± 2.32	18.46 ± 0.92	48.92 ± 2.4
WE	0.162 ± 0.008	47.78 ± 2.38	15.58 ± 0.77	64.08 ± 3.2

Characterization Techniques Used

Morphological Analysis

The morphology of the biosynthesized AgNPs was characterized by TEM. The prepared AgNPs solution was sonicated in hot water for 30 min. The prepared sample one drop was placed on carbon-sputtered copper grids and allowed to dry. TEM analysis was performed by the JEM-2100F instrument at the voltage of 200 kV. AgNPs incorporated (WE) film surface morphology and dispersion of nanoparticles was characterized by the FE- SEM Model JEOL 7610F. AFM images of WE film were taken by Alpha 300 RA AFM & RAMAN at scan rate 1 Hz and tapping mode used.

Spectrophotometry Analysis

Bio reduced AgNPs and SA composite films were characterized by the instrument Cary 5000 UV–Vis–NIR spectrophotometer (scanning range 200–800 nm). Equal amounts of the solution (2.5 mL) were taken and the film sample was taken directly and the entire sample was analyzed at room temperature. The FTIR measurements were taken by SPECTRUM 400 scan range 4000 to 400 cm⁻¹, AgNPs solution was taken directly and similarly, WE film also analyzed to identify the chemical structure and potential interactions between sodium alginate and AgNPs.

Contact Angle Measurement

The contact angle measurement was characterized by SEO Phoenix. For this, the prepared alginate and AgNPs incorporated films cut into 1 × 3 cm pieces and positioned on the stage. The sessile drop method was performed, DI water using as a reference liquid.

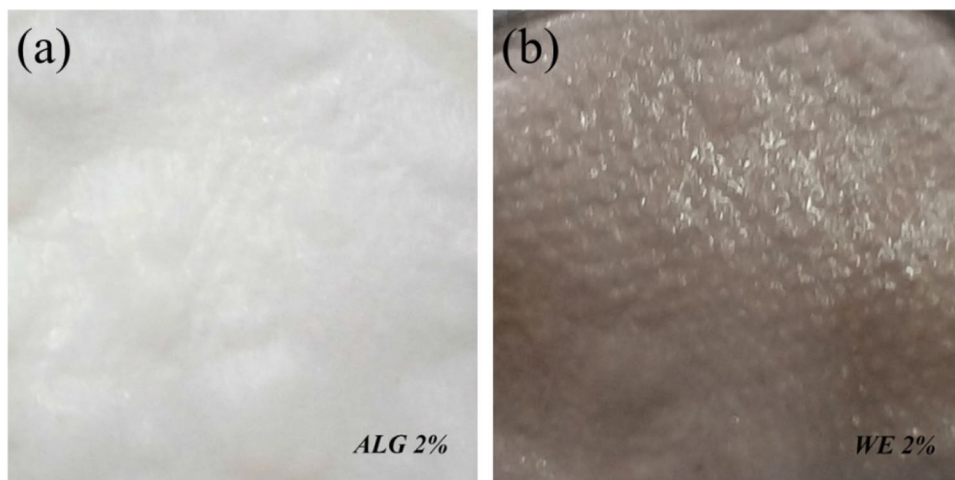
Mechanical Strength

The mechanical properties of ALG and WE films were measured using UTM (Tinius Olsen) model H 50 KT, size of film samples were used 1 × 3 cm at 1 mm/min crosshead speed using 100 N load cell. By analyzing the elongation break percentage, tensile strength and Young's modulus are measured.



Fig. 2 A schematic diagram of sodium alginate and AgNPs incorporated films preparation

Fig. 3 Optical images of prepared a neat sodium alginate (ALG) and b AgNPs incorporated alginate (WE) films



Films Physical Properties

Film thickness was measured by a digital vernier calliper with 0.001 mm accuracy, for each film sample, five readings were taken at different positions.

For the Water Sensitivity Tests

To measure the moisture content of the films, samples were initially weighed (M_0) and then dried in a hot air oven at 105

$^{\circ}\text{C}/24\text{ h}$ (M_1). Total moisture content was measured by the equation following equation;

$$\text{Moister content}(\omega) = \frac{M_1}{M_0} \times 100 \tag{1}$$

All film samples were dried in a hot air oven for removing the moisture at 105 $^{\circ}\text{C}$ for 24 h. After that, the dried films were weighed for initial mass (W_0), to measure the water solubility the dried films were immersed in distilled water

and placed on the magnetic stirrer (100 rpm) at 25 °C for 24 h. Then the films were again dried in a hot air oven at 105 °C for 24 h for taking final weight (W_f) of the films.

$$\text{Water soluble(WS)} = \frac{W_0 - W_f}{W_0} \times 100 \quad (2)$$

For swelling and absorption studies, the dried films were kept in DI water at room temperature. The wet samples were taken out and removed the excess water with the help of filter paper and reweighed (W_f). For swelling studies, different time intervals were considered and for absorption studies only 24 h required. The amount of the water absorbance was calculated by the given equation;

$$\text{Swelling and absorption} = \frac{W_f - W_0}{W_0} \times 100 \quad (3)$$

where W_0 is an initial weight and W_f is the final weight.

Antimicrobial Activity

Antimicrobial activity of the both biosynthesized AgNPs from plant extract and AgNPs incorporated sodium alginate (WE) film was examined for their inhibitory effects on the growth of the microorganisms. The antimicrobial study was evaluated using two types of bacteria such as *Escherichia*

coli (Gram-negative) and *Staphylococcus aureus* (Gram-positive). The microbial study was investigated by two methods such as nutrient agar well diffusion method for AgNPs and disc diffusion method for WE composite film. The tested microorganisms were swabbed uniformly on nutrient agar-agar plates using the sterile cotton swab and 4 wells were created on every plate with 6 mm diameter. The prepared AgNPs were poured into wells of 25 μ l, 50 μ l, 75 μ l and 100 μ l concentration of solutions. Similarly, AgNPs loaded composite film cut into small pieces and placed on the swabbed surface of the plate. Then the agar plates were incubated at 37 °C/24 h for growing microorganism and bacteria cultures. Finally, the diameter of zone inhibition (ZOI) was measured.

Result and Discussion

Morphological Studies

HR-TEM is a widely used technique to measure the nanoparticle size, and it provides information on the morphology of nanoparticles. The surface morphology of bioreduced AgNPs from *Nymphae odorata* plant extract images are shown in Fig. 4. It was observed that the synthesized AgNPs in a spherical shape and the particle size range

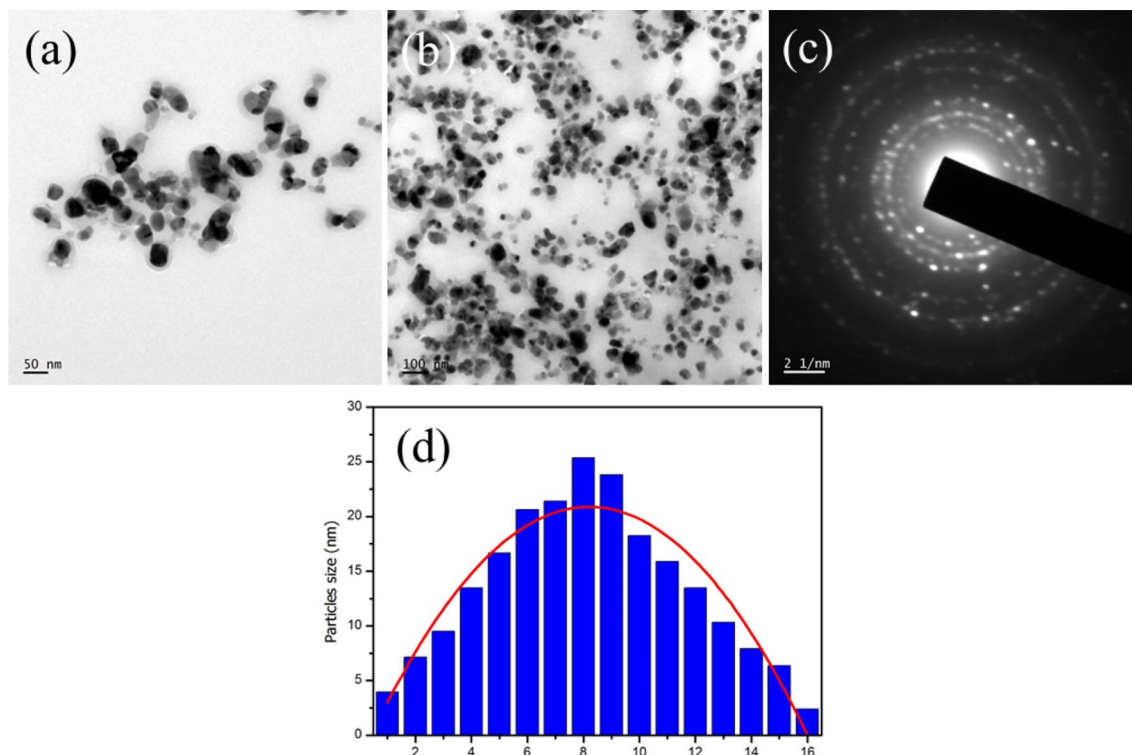


Fig. 4 HR-TEM images **a**, **b** of AgNPs from plant extract, **c** SEAD pattern shows the crystalline nature of the AgNPs and **d** Image J graph showed the particle size

is 15 ± 5 nm. In Fig. 4d *Image J* analyzer has revealed the diameter of NPs of approximately 20 nm. Figure 4c shows SEAD patron of AgNPs which showed the crystalline nature of NPs. Also, the TEM images depict that the maximum number of AgNPs approximately having a spherical shape with soft boundaries and few NPs have anisotropic structures with asymmetrical counters. It can be seen that most of the AgNPs are in close physical contact but separated by uniform interparticle distance [44]. The NPs were enclosed with other materials by pale light layer, it is because that the plant extract has also worked as a capping agent. In the TEM images, it is evident that the biosynthesized AgNPs does not show any aggregation [45].

SEM technique has revealed about the dispersion of NPs, size, surface morphology and the difference in the film morphology due to the cross-linking. By this technique, biosynthesized WE film was analyzed and the result is shown in Fig. 5. The WE film was showed a rough surface and uniform dispersion of AgNPs on the polymer matrix. As we can observe that the alginate film surface was mostly covered with AgNPs. Moreover, AgNPs size was increased in the polymer matrix, because of the surface of the particles was coated with alginate. The morphology also exhibited the existence of AgNPs with dissimilar shape and some aggregation in the film surface [46, 47].

Topographical images of WE film was performed by AFM to observe the surface roughness, presence of particles, dispersion and the size of AgNPs. The surface topography of the prepared AgNPs loaded film image is shown in Fig. 6. The direct observation of the AFM image showed the size of the NPs of about 21 nm. From the 3D image, it exhibited the uniform growth direction of the particles and it was demonstrated that the AgNPs well-dispersed on the film surface. The obtained data from AFM was well corroborated with our TEM and SEM analysis. The fabricated film morphology depended on different factors like polymer solubility, the composition of the surface, solvent evaporation, molecular weight and thickness [48].

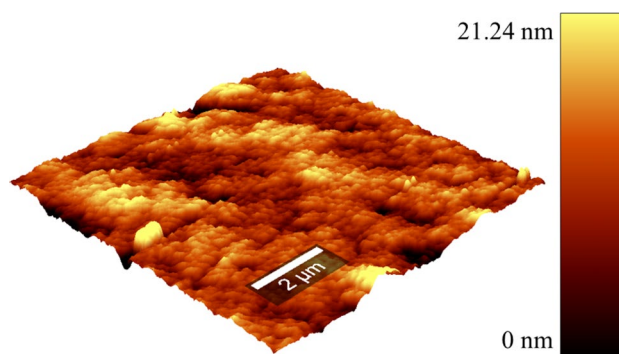


Fig. 6 3D morphology of AgNPs incorporated film

Spectroscopy Analysis

AgNPs were formed by the reduction of Ag^+ into Ag^0 with the addition of *Nymphae odorata* extract to the 1 mM silver nitrate solution. UV–visible absorption spectroscopy is a good technique to demonstrate the presence of NPs. Figure 7a shows the UV spectrum of prepared AgNPs. Here plant extract act as both capping and reducing agent, AgNPs exhibits yellowish-brown due to excitation of SPR (surface plasmon resonance) in AgNPs. It is well known that any type of plant extracts mixed with silver nitrate we can observe the colour changes which indicates the development of AgNPs. Most of the literature reported the reaction between AgNO_3 and plant extract [49, 50]. AgNPs have electron density around them, which gives rise to SPR absorption band, due to the combined vibration of AgNPs in resonance with the light wave. Previous studies have been shown that the NPs in spherical shapes contribute the absorption bands at 400–420 nm [51]. AgNPs UV spectrophotometer gives the λ_{max} value at 400–430 nm. The UV spectrum of AgNPs has a sharp absorbance peak at 415 nm. The absorbance peak increases with increasing the reduction time, the colour changes were observed from yellow to reddish-brown and this colour was stable. This colour deviation caused by the excitation of a metal nanoparticle of SPR. The broad absorption peak at 400–430 nm obtained between 10 and 40 min reaction

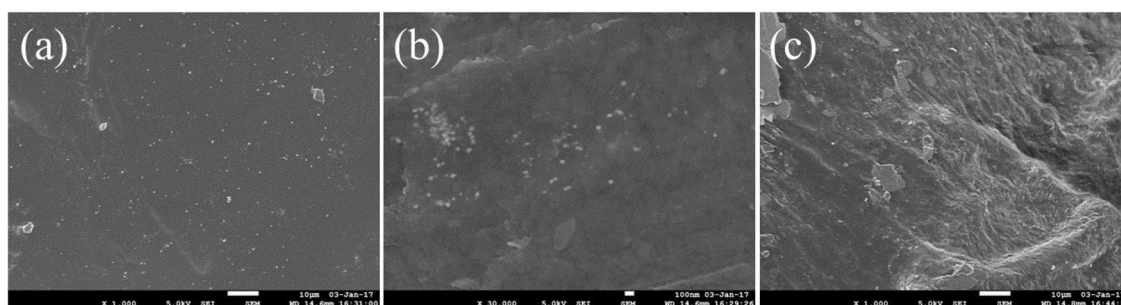


Fig. 5 FE-SEM micrographs of WE composite film a, b AgNPs incorporated Alginate film, c cross-section

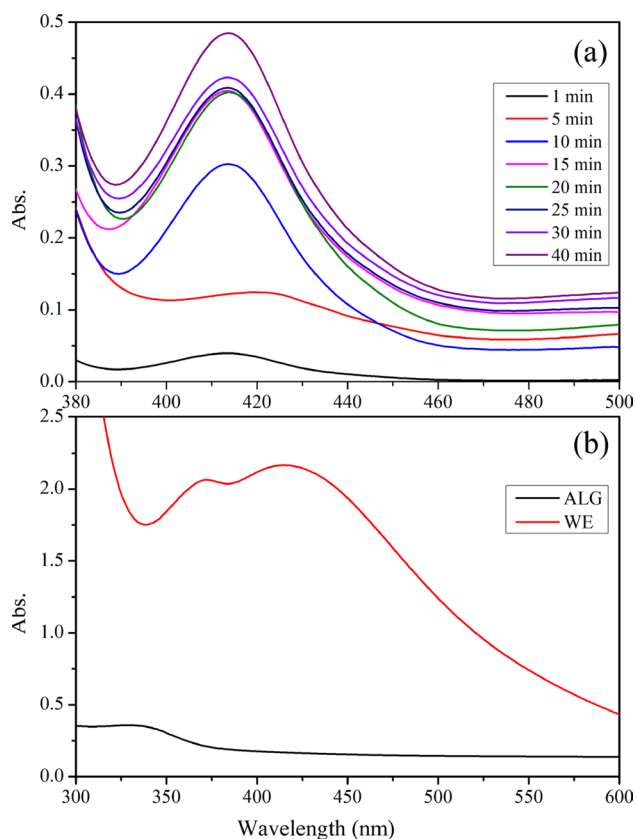


Fig. 7 UV peak absorbance of **a** biosynthesized silver nanoparticles in different periods, **b** Alginate and AgNPs incorporated films

time becomes narrow as the time of reaction increased with increase in absorbance spectra. As the reaction time is prolonged there will be an increase in the number of particles present in the solution with uniform size distribution [9]. To understand this phenomenon, a schematic representation of surface plasmon oscillation under the effect of an electromagnetic field and surface plasmon vibrations excitation of AgNPs was reported in Ref. [52].

UV absorption and transmission spectrum of prepared WE film was also characterized by a spectrophotometer in the range of UV visible light. The present technique was used to observe the silver peak in WE composite film and their absorption and transmission spectrum (Fig. 7b). WE composite film exhibited absorption band of AgNPs wavelength at 420 nm, which is a typical SPR band and it showed that the presence of NPs on the composite film. The control composite film did not show any absorbance/transmittance values.

In the present study, the IR spectrum was performed to identify the functional groups of biosynthesized AgNPs and interaction of silver nitrate and phytochemicals (Fig. 8a). AgNPs showed intensive peaks at 3325, 2110, 1634, 1365 and 1216 cm^{-1} . The peak at 3325 cm^{-1} showed the presence

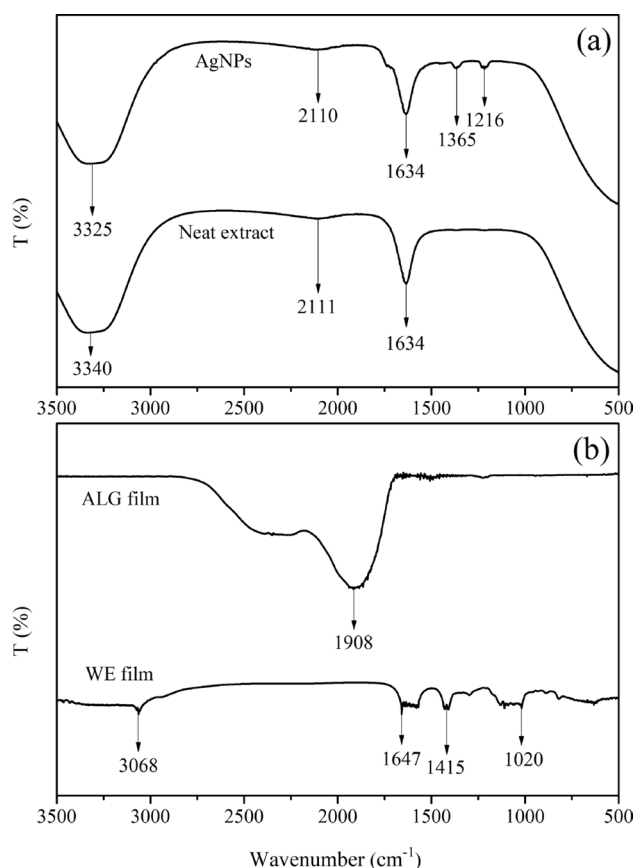


Fig. 8 FTIR analysis of **a** AgNPs from plant extract, **b** peak information of alginate and AgNPs incorporated films

of O–H groups, 2110 cm^{-1} shows the presence of C \equiv C Terminal alkyne, 1634 cm^{-1} are the stretching vibrations of C=O, C=C and carbonyl group. The band appearing at 1365 cm^{-1} was due to the presence of C–O ester sulfate group, and 1216 cm^{-1} exhibits the presence of C–H aromatic group. The peak shift and intensity distribution were also studied. The present result suggests that the proteins are interacting with the AgNPs and also the structures were not be affected by the reaction with Ag⁺ ion after binding with AgNPs. FTIR study recommended that the hydroxyl groups of phenols and amide groups of proteins from plant extract forming a layer to the NPs and acts as a capping agent. Also, it gives stability and prevents agglomeration in the medium [15, 53].

FTIR spectrum of prepared composites such as neat alginate and AgNPs incorporated alginate films exhibited distinctive peaks in the range of 4000–400 cm^{-1} . The interaction between the alginate and AgNPs were identified and it is shown in Fig. 8b. FTIR analysis of pure alginate (ALG) film shown the absorption peak at 1908 cm^{-1} and this peak corresponds to an asymmetric C=C band. The WE film spectrum showed the presence of peaks at 1647, 1415 and 1020 cm^{-1} . The peak around 1647 cm^{-1} is the stretching vibration of the

conjugated peptide band formation of (NH₂) amine group. The band at 1415 cm⁻¹ corresponds to the –OH group of the primary alcoholic group. The sharp absorption peak at 1020 cm⁻¹ is attributed to the C–N stretching vibration of aliphatic amines or alcohols or phenols representing the presence of polyphenols.

Contact Angle

The water contact angle was carried out to measure the hydrophilicity/hydrophobicity of ALG and WE film, the degree of contact angles is shown in Fig. 9. ALG film contact angle was 42°, which indicates the film surface having hydrophilic nature because it contained a huge quantity of carboxyl and hydroxyl groups. For the AgNPs incorporated WE film contact angle displays 54°, this was the good indication when compared to ALG film and it clears that the WE film has better contact angle after adding NPs. The contact angle of the ALG film was not changed significantly when AgNPs incorporated into the alginate film angle increased considerably. The increased contact angle of WE composite was mainly due to the AgNPs hydrophobic metallic nature of silver [54].

Mechanical Analysis

The mechanical properties of the polymer composite films are usually measured by the tensile strength, elongation at break and modulus. These are generally used to calculate the film flexibility, strength and stiffness. Mechanical properties are an important characterization technique for testing films and it could be used as an indicator of the film to maintain the strength, integrity and towards resisting ecological stress throughout various applications. The stress–strain curve behaviour of the ALG and WE films are shown in Fig. 10. ALG film shows high tensile strength 29.1 ± 1.4 MPa and low elongation at break 1.3 ± 0.06 . WE film shown 17.6 ± 0.9 MPa tensile strength and elongation at break 9.01 ± 0.9 . The tensile strength of WE compared was with ALG film and it exhibits the strength of the WE film was significantly decreased. The decreased tensile strength

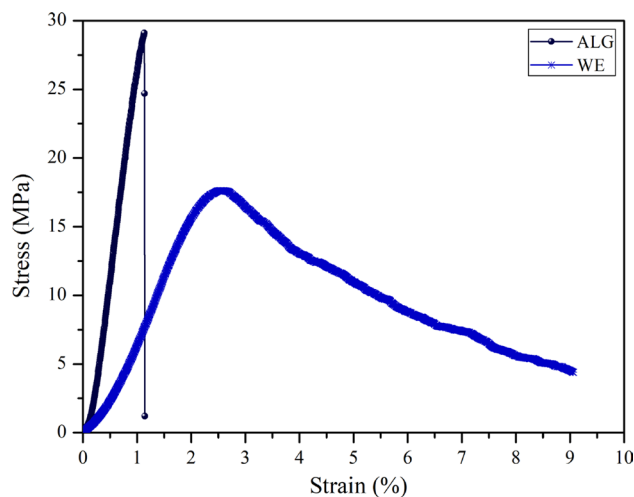


Fig. 10 Stress–strain curves of the prepared composite films

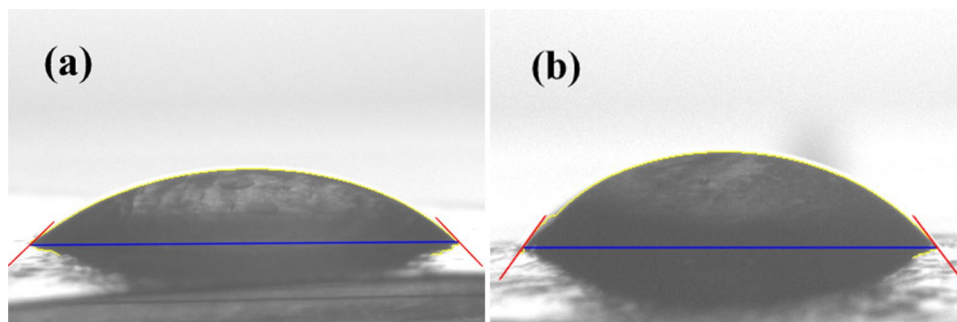
at high concentration was due to the formation of voids and cracks in the polymer matrix caused by the agglomeration of NPs and at the same time elongation was increased. This might be caused by the reduction in intra and inter-molecular chain interaction of alginate due to the incorporation of AgNPs. The addition of AgNPs into these films reduces the interaction between the polymer chains as large numbers of –OH groups and –COOH groups of alginate is presumably complexed with AgNPs and will not be available for the polymer–polymer interaction. Similar mechanical properties were reported by Shankar et al. [55] with agar/AgNPs and gelatin/AgNPs composite films. The presence of AgNPs imparts increased elongation at break with compromising the tensile strength. This result shows the good flexibility of the developed composites.

Physical Properties of Films

Film Thickness

Thin films were obtained by mixing of alginate and AgNPs solution and cast on the mould. The ALG film was appeared

Fig. 9 Contact angle measurement of the films **a** Neat alginate, **b** AgNPs incorporated



to be grey in colour and the WE film showed a light brown colour (Fig. 3). ALG film thickness was 0.174 mm and WE film was 0.162 mm, ALG film has the highest thickness when compared to WE film. It means ALG film has more alginate concentration so the thickness was increased and WE film has less thickness when compared with ALG as you can see in Table 1. This was attributed to the degradation of alginate and the strong interaction of both ALG and WE composite films.

Water Sensitivity Tests

Films moisture content was reported in Table 1. Both composite films had similar moisture contents and after the incorporation of AgNPs, there was a slight increase in the moisture percentage. The water content of the ALG film 46.5 ± 2.3 after incorporation of AgNPs moisture content slightly increased. This was due to the strong interaction between AgNPs and alginate polymer matrix. This was also observed in the mechanical properties.

ALG and WE film water solubility were determined to evaluate the water resistance and it is the essential application for drug release studies. The solubility of ALG film (18%) was found to be higher when compared to WE film (15%). The solubility of ALG films was increased due to the presence of hydrophilic groups. After incorporation of AgNPs solubility of the film slightly decreased, it was around 15%. This was because of the formation of AgNPs between bound Ag^+ ions and carboxyl groups on the surface of the WE film. The film samples water solubility was determined for 24 h at 37 °C.

Table 1 reported that the water absorption capacity values of the film, ALG film has shown 48% swelling and the WE film showed about 64%. After incorporation of AgNPs into film water absorption increased, the results showed that the film capacity to absorb water is dependent on the pH value of the medium and the decrease of pH is associated with a decrease in the films' water uptake. Alginate is protonated into insoluble forms of alginic acid at lower pH values, which influences the swelling degree. AgNPs incorporation into the SA film contributes to a slight increase in the films water uptake for DI water media [56, 57].

Alginate films were subjected to swelling studies with distilled water at room temperature. The stability was evaluated and as well as the water uptake capacity of the AgNPs incorporated alginate composite in aqueous media. The data obtained over a large time period of swelling values, are reported in Table 2. The ALG film swelling ratios gradually increased with respect to the time period but it showed less swelling behaviour when compared with AgNPs incorporated film. Both ALG and WE composite films at day 7 slightly dissolved in water and also WE film absorbed highest 130.2%. ALG film showed maximum 117.2% at day 5

Table 2 Water swelling degree of prepared composite films

Samples	Day 1	Day 2	Day 5	Day 7
ALG	48.9	97.8	117.2	105.9
WE	64	73.2	81.6	130.2

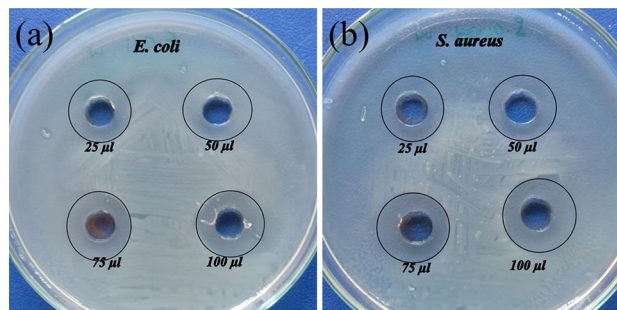


Fig. 11 Biosynthesized AgNPs microbial activity at different concentration

after that it gradually lost the water uptake capacity also stability.

Antimicrobial Study

Many researchers have been reported that the biosynthesis of AgNPs from plant extracts including Tulsi [58], Lemongrass [59], and Banana peel [60] etc. [11, 61]. Biosynthesized AgNPs antimicrobial activity was evaluated by well diffusion method and *Escherichia coli*, *Staphylococcus aureus* pathogenic microorganisms were used. The antibacterial activity of AgNPs was good and evaluated by the zone of inhibition (ZOI) (Fig. 11). Table 3 indicated that the large ZOI was formed with an increase in the concentration of AgNPs. ZOI diameter of *E. coli*, *S. aureus* was (14–16 mm) and (16–18 mm), respectively. The high bactericidal activity of AgNPs is caused by their particularly bigger shell region which provides improved interaction with the bacteria [62]. Moreover, AgNPs work as reservoirs for the Ag^+ as bactericidal agent [60].

The antibacterial activities of SA composite films were characterized by disc diffusion method, two types of microorganisms used such as *S. aureus* and *E. coli*. The activity was evaluated by measuring the ZOI (Fig. 12). According to the obtained result, WE film showed increased activity, it might be due to the interaction between the positive charge of the alginate with the negative charge on the cell member of the bacterium, causing the leakage of intermolecular constituents and cell death [63]. WE film shown good antimicrobial activity against two pathogenic bacteria and ZOI of *E. coli* was 14 ± 0.07 mm and *S. aureus* was 13 ± 0.06 mm. It was based on the measurement of the ZOI caused by the

Table 3 Zone of inhibition measurements of the silver nanoparticles at different concentrations

<i>E. coli</i>				<i>S. aureus</i>			
25 μ l	50 μ l	75 μ l	100 μ l	25 μ l	50 μ l	75 μ l	100 μ l
15 \pm 0.07	16 \pm 0.08	17 \pm 0.08	18 \pm 0.9	15 \pm 0.07	16 \pm 0.08	19 \pm 0.09	20 \pm 0.1

antimicrobial agent present in the film [64, 65]. The main mechanism is that the metallic AgNPs act together with the outer membrane of bacteria causing structural changes and distraction of the bacteria. And another reason is that AgNPs due to its smaller particle size, it easily penetrates the bacterial cell more effectively. Thus, AgNPs prepared by natural medicinal plants extract might be a good antibacterial bio-resource with potential application in biomedical and the related areas.

Conclusions

In this study, we have developed a low-cost, one step and eco-friendly method as per the green chemistry principles and it is represented as a non-toxic method. The present report emphasizes the use of phytochemicals for AgNPs synthesis as well as the incorporation of AgNPs into the SA films. Alginate plays a vital role, it works as Ag⁺ reducing and stabilizing agent, but in the present work, we used as a polymer matrix. The prepared AgNPs incorporated into SA film were characterized by physicochemical methods. Mechanical properties and water sensitivity properties have been enhanced after the formation of alginate composite with AgNPs. Because of the proper selection of AgNPs as filler on the polymer matrix, they showed improvement in the water sensitivity, mechanical properties as well as it has an excellent antimicrobial activity. The prepared composite film showed excellent antimicrobial activity against two microorganisms such as *E. coli* and *S. aureus*. The present approach of synthesis of Ag NPs utilized green chemistry principles and thus, films prepared from as-synthesized NPs can potentially be used for food packaging, like wound

dressings, graftings onto various implants and several other biotechnological and biomedical applications.

Acknowledgements This work was as a part of M.Sc. Project work of Mr. Apparao Gudimalla and self-funded research. AG wants to express his thanks to Ms. Rajakumari R and Ms. Merina Luke for the valuable discussions and assistance in diffusion experiments during the course of the work.

Author Contributions AG and JJ conceived and designed the research work. AG conducted all experiments, characterizations and wrote the manuscript. JJ, JV and ST contributed the lab facilities, reagents and analytical tools as well as supervised the research. All authors read and approved the manuscript.

Compliance with Ethical Standards

Conflict of interest The authors have no potential conflicts of interest to disclose.

Research Involving Human and Animal Rights This article does not contain any studies with human participants or animals performed by any of the authors.

References

1. Laurencin CT, Kumbar SG, Nukavarapu SP (2009) Nanotechnology and orthopedics: A personal perspective. Wiley Interdiscip Rev Nanomedicine Nanobiotechnology 1:6–10. doi:<https://doi.org/10.1002/wnan.25>
2. Rodríguez-Luis O, Hernandez-Delgadillo R Green (2016) Synthesis of silver nanoparticles and their bactericidal and antimycotic activities against oral microbes. J Nanomater
3. Barabadi H (2017) Nanobiotechnology: a promising scope of gold biotechnology. Cell Mol Biol 63:3–4. doi:<https://doi.org/10.14715/cmb/2017.63.12.2>
4. Shi J, Kantoff PW, Wooster R (2017) Farokhzad OC cancer nanomedicine: progress, challenges and opportunities. Nat Rev Cancer 17:20–37. <https://doi.org/10.1038/nrc.2016.108>
5. Vijayakumar M, Priya K, Nancy FT, Noorlidah A, Ahmed ABA (2013) Biosynthesis, characterisation and anti-bacterial effect of plant-mediated silver nanoparticles using *Artemisia nilagirica*. Ind Crops Prod 41:235–240. <https://doi.org/10.1016/j.indcrop.2012.04.017>
6. Franci G, Falanga A, Galdiero S, Palomba L, Rai M, Morelli G, Galdiero M (2015) Silver nanoparticles as potential antibacterial agents. Molecules 20:8856–8874. doi:<https://doi.org/10.3390/molecules20058856>
7. Muthukumar U, Govindarajan M, Rajeswary M, Hoti SL (2015) Synthesis and characterization of silver nanoparticles using *Gmelina asiatica* leaf extract against filariasis, dengue, and malaria vector mosquitoes. Parasitol Res 114:1817–1827. <https://doi.org/10.1007/s00436-015-4368-4>

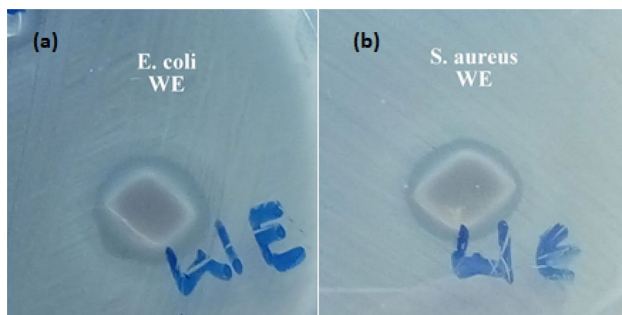


Fig. 12 Antimicrobial activity of silver nanoparticles incorporated alginate film against *E. coli* and *S. aureus*

8. Tetgure SR, Borse AU, Sankapal BR, Garole VJ, Garole DJ (2015) Green biochemistry approach for synthesis of silver and gold nanoparticles using *Ficus racemosa* latex and their pH-dependent binding study with different amino acids using UV/Vis absorption spectroscopy. *Amino Acids* 47:757–765. <https://doi.org/10.1007/s00726-014-1906-9>
9. Jemilugba OT, Sakho EHM, Parani S, Mavumengwana V, Oluwafemi OS (2019) Green synthesis of silver nanoparticles using *Combretum erythrophyllum* leaves and its antibacterial activities. *Colloids Interface Sci Commun.* <https://doi.org/10.1016/j.colcom.2019.100191>
10. Masurkar SA, Chaudhari PR, Shidore VB, Kamble SP (2011) Rapid biosynthesis of silver nanoparticles using *Cymbopogon Citratus* (Lemongrass) and its antimicrobial activity. *Nano-Micro Lett* 3:189–194. <https://doi.org/10.3786/nml.v3i3.p189-194>
11. Ahmed S, Ahmad M, Swami BL, Ikram S (2016) A review on plants extract mediated synthesis of silver nanoparticles for antimicrobial applications: a green expertise. *J Adv Res* 7:17–28. <https://doi.org/10.1016/j.jare.2015.02.007>
12. Duan H, Wang D, Li Y (2015) Green chemistry for nanoparticle synthesis. *Chem Soc Rev.* doi:<https://doi.org/10.1039/c4cs00363b>
13. Jose Varghese R, Zikalala N, Sakho EHM, Oluwafemi OS (2020) Green synthesis protocol on metal oxide nanoparticles using plant extracts. In: *Colloidal metal oxide nanoparticles*
14. Krishnaraj C, Jagan EG, Rajasekar S, Selvakumar P, Kalaichelvan PT, Mohan N (2010) Synthesis of silver nanoparticles using *Acalypha indica* leaf extracts and its antibacterial activity against water borne pathogens. *Colloids Surf B* 76:50–56. <https://doi.org/10.1016/j.colsurfb.2009.10.008>
15. Yugandhar P, Haribabu R, Savithamma N (2015) Synthesis, characterization and antimicrobial properties of green-synthesised silver nanoparticles from stem bark extract of *Syzygium alternifolium* (Wt.) Walp. *3 Biotech* 5:1031–1039. <https://doi.org/10.1007/s13205-015-0307-4>
16. Garg S, Chandra A, Mazumder A, Mazumder R (2014) Green synthesis of silver nanoparticles using *Arnebia nobilis* root extract and wound healing potential of its hydrogel. *Asian J Pharm* 8:95. <https://doi.org/10.4103/0973-8398.134925>
17. Sundaravadevelan C, Nalini Padmanabhan M, Sivaprasath P, Kishmu L (2013) Biosynthesized silver nanoparticles from *Pedilanthus tithymaloides* leaf extract with anti-developmental activity against larval instars of *Aedes aegypti* L. (Diptera; Culicidae). *Parasitol Res* 112:303–311. <https://doi.org/10.1007/s00436-012-3138-9>
18. Dipankar C, Murugan S, Colloids, Surfaces B (2012) Biointerfaces The green synthesis, characterization and evaluation of the biological activities of silver nanoparticles synthesized from *Iresine herbstii* leaf aqueous extracts. *Colloids Surf B* 98:112–119. <https://doi.org/10.1016/j.colsurfb.2012.04.006>
19. Vasanth K, Ilango K, MohanKumar R, Agrawal A, Dubey GP (2014) Anticancer activity of *Moringa oleifera* mediated silver nanoparticles on human cervical carcinoma cells by apoptosis induction. *Colloids Surf B* 117:354–359. <https://doi.org/10.1016/j.colsurfb.2014.02.052>
20. Maruti C, Kumar K, Yugandhar P, Sührulatha D, Savithamma N (2015) Synthesis, characterization and antimicrobial studies of stem bark mediated synthesis of silver nanoparticles from *Adansonia digitata* (L.). *J Pharm Sci Res* 7:76–82
21. Mohamed El-Rafie H, Abdel-Aziz Hamed M (2014) Antioxidant and anti-inflammatory activities of silver nanoparticles biosynthesized from aqueous leaves extracts of four Terminalia species. *Adv Nat Sci Nanosci Nanotechnol* 5:035008. <https://doi.org/10.1088/2043-6262/5/3/035008>
22. Krithiga N, Rajalakshmi A, Jayachitra A (2015) Green synthesis of silver nanoparticles using leaf extracts of *Clitoria ternatea* and *Solanum nigrum* and study of its antibacterial effect against common nosocomial Pathogens
23. Singh A, Jain D, Upadhyay MK, Khandelwal N (2010) Green synthesis of silver nanoparticles using Argemone mexicana leaf extracts and evaluation of their antimicrobial activities. *Dig J Nanomater Biostruct* 5:483–489
24. Velusamy P, Su CH, Kumar GV, Adhikary S, Pandian K, Gopinath SCB, Chen Y, Anbu P (2016) Biopolymers regulate silver nanoparticle under microwave irradiation for effective antibacterial and antibiofilm activities. *PLoS ONE* 11:1–14. <https://doi.org/10.1371/journal.pone.0157612>
25. Azlin-Hasim S, Cruz-Romero MC, Cummins E, Kerry JP, Morris MA (2016) The potential use of a layer-by-layer strategy to develop LDPE antimicrobial films coated with silver nanoparticles for packaging applications. *J Colloid Interface Sci* 461:239–248. doi:<https://doi.org/10.1016/j.jcis.2015.09.021>
26. Ionita M, Pandele MA, Iovu H (2013) Sodium alginate/graphene oxide composite films with enhanced thermal and mechanical properties. *Carbohydr Polym* 94:339–344. doi:<https://doi.org/10.1016/j.carbpol.2013.01.065>
27. Rani P, Mishra S, Sen G (2013) Microwave based synthesis of polymethyl methacrylate grafted sodium alginate: Its application as flocculant. *Carbohydr Polym* 91:686–692. doi:<https://doi.org/10.1016/j.carbpol.2012.08.023>
28. Deepa B, Abraham E, Pothan LA, Cordeiro N, Faria M, Thomas S (2016) Biodegradable nanocomposite films based on sodium alginate and cellulose nanofibrils. *Materials* 9:1–11. <https://doi.org/10.3390/ma9010050>
29. Puppi D, Zhang X, Yang L, Chiellini F, Sun X, Chiellini E (2014) Nano/microfibrous polymeric constructs loaded with bioactive agents and designed for tissue engineering applications: A review. *J Biomed Mater Res - Part B Appl Biomater* 102:1562–1579. doi:<https://doi.org/10.1002/jbm.b.33144>
30. Martins M, Barros AA, Quraishi S, Gurikov P, Raman SP, Smirnova I, Duarte ARC, Reis RL (2015) Preparation of macroporous alginate-based aerogels for biomedical applications. *J Supercrit Fluids* 106:152–159. doi:<https://doi.org/10.1016/j.supflu.2015.05.010>
31. Dumitriu RP, Oprea AM, Natalia Cheaburu C, Nistor MT, Novac O, Ghiciuc CM, Profire L, Vasile C (2014) Biocompatible and biodegradable alginate/poly(N-isopropylacrylamide) hydrogels for sustained theophylline release. *J Appl Polym Sci* 131:8939–8954. doi:<https://doi.org/10.1002/app.40733>
32. Daemi H, Barikani M, Sardon H (2017) Transition-metal-free synthesis of supramolecular ionic alginate-based polyurethanes. *Carbohydr Polym* 157:1949–1954. doi:<https://doi.org/10.1016/j.carbpol.2016.11.086>
33. Galus S, Lenart A (2013) Development and characterization of composite edible films based on sodium alginate and pectin. *J Food Eng* 115:459–465. doi:<https://doi.org/10.1016/j.jfoodeng.2012.03.006>
34. Karakasyan C, Mathos J, Lack S, Davy J, Marquis M, Renard D (2015) Microfluidics-assisted generation of stimuli-responsive hydrogels based on alginates incorporated with thermo-responsive and amphiphilic polymers as novel biomaterials. *Colloids Surf B* 135:219–629. <https://doi.org/10.1016/j.colsurfb.2015.08.028>
35. Kulkarni RV, Boppana R, Krishna Mohan G, Mutalik S, Kalyane NV (2012) PH-responsive interpenetrating network hydrogel beads of poly(acrylamide)-g-carrageenan and sodium alginate for intestinal targeted drug delivery: synthesis, in vitro and in vivo evaluation. *J Colloid Interface Sci* 367:509–517. <https://doi.org/10.1016/j.jcis.2011.10.025>
36. Olivas GI, Barbosa-Cánovas GV (2008) Alginate-calcium films: water vapor permeability and mechanical properties as affected by plasticizer and relative humidity. *LWT-Food Sci Technol* 41:359–366. <https://doi.org/10.1016/j.lwt.2007.02.015>

37. Orsuwan A, Shankar S, Wang LF, Sothornvit R, Rhim JW (2016) Preparation of antimicrobial agar/banana powder blend films reinforced with silver nanoparticles. *Food Hydrocoll* 60:476–485. doi:<https://doi.org/10.1016/j.foodhyd.2016.04.017>
38. Wang J, Wei J, Su S, Qiu J, Wang S (2015) Ion-linked double-network hydrogel with high toughness and stiffness. *J Mater Sci* 50:5458–5465. doi:<https://doi.org/10.1007/s10853-015-9091-0>
39. Liu Y, Zhao JC, Zhang CJ, Guo Y, Zhu P, Wang DY (2016) Effect of manganese and cobalt ions on flame retardancy and thermal degradation of bio-based alginate films. *J Mater Sci* 51:1052–1065. doi:<https://doi.org/10.1007/s10853-015-9435-9>
40. Duceppe N, Tabrizian M (2010) Advances in using chitosan-based nanoparticles for in vitro and in vivo drug and gene delivery. *Expert Opin Drug Deliv* 7:1191–1207. doi:<https://doi.org/10.1517/17425247.2010.514604>
41. Meng X, Tian F, Yang J, He CN, Xing N, Li F (2010) Chitosan and alginate polyelectrolyte complex membranes and their properties for wound dressing application. *J Mater Sci Mater Med* 21:1751–1759. doi:<https://doi.org/10.1007/s10856-010-3996-6>
42. Ma S, Chen Z, Qiao F, Sun Y, Yang X, Deng X, Cen L, Cai Q, Wu M, Zhang X et al (2014) Guided bone regeneration with triphosphate cross-linked asymmetric chitosan membrane. *J Dent* 42:1603–1612. doi:<https://doi.org/10.1016/j.jdent.2014.08.015>
43. Sikareepaisan P, Ruktanonchai U, Supaphol P (2011) Preparation and characterization of asiaticoside-loaded alginate films and their potential for use as effectual wound dressings. *Carbohydr Polym* 83:1457–1469. doi:<https://doi.org/10.1016/j.carbpol.2010.09.048>
44. Edison TNJI, Lee YR, Sethuraman MG (2016) Green synthesis of silver nanoparticles using *Terminalia cuneata* and its catalytic action in reduction of direct yellow-12 dye. *Spectrochim Acta Part A* 161:122–129. <https://doi.org/10.1016/j.saa.2016.02.044>
45. Ren Y, Yang H, Wang T, Wang C (2016) Green synthesis and antimicrobial activity of monodisperse silver nanoparticles synthesized using *Ginkgo Biloba* leaf extract. *Phys Lett Sect A* 380:3773–3777. <https://doi.org/10.1016/j.physleta.2016.09.029>
46. Kanmani P, Rhim JW (2014) Properties and characterization of bionanocomposite films prepared with various biopolymers and ZnO nanoparticles. *Carbohydr Polym* 106:190–199. doi:<https://doi.org/10.1016/j.carbpol.2014.02.007>
47. Bierhalz ACK, da Silva MA, Braga MEM, Sousa HJC, Kieckbusch TG (2014) Effect of calcium and/or barium crosslinking on the physical and antimicrobial properties of natamycin-loaded alginate films. *LWT-Food Sci Technol* 57:494–501. <https://doi.org/10.1016/j.lwt.2014.02.021>
48. Ahmad MB, Lim JJ, Shamel K, Ibrahim NA, Tay MY (2011) Synthesis of silver nanoparticles in chitosan, gelatin and chitosan/gelatin bionanocomposites by a chemical reducing agent and their characterization. *Molecules* 16:7237–7248. doi:<https://doi.org/10.3390/molecules16097237>
49. Namratha N, Monica PV (2013) Synthesis of silver nanoparticles using *Azadirachta indica* (Neem) extract and usage in water purification. *Asian J Pharm Technol* 3:170–174
50. Lalitha A, Subbaiya R, Ponmurugan P (2013) Green synthesis of silver nanoparticles from leaf extract *Azadirachta indica* and to study its anti-bacterial and antioxidant property. *Int J Curr Microbiol Appl Sci* 2:228–235
51. Suman TY, Radhika Rajasree SR, Kanchana A, Elizabeth SB (2013) Biosynthesis, characterization and cytotoxic effect of plant mediated silver nanoparticles using *Morinda citrifolia* root extract. *Colloids Surf B* 106:74–78. <https://doi.org/10.1016/j.colsurfb.2013.01.037>
52. Barabadi H, Honary S, Ebrahimi P, Alizadeh A, Naghibi F, Saravanan M (2019) Optimization of myco-synthesized silver nanoparticles by response surface methodology employing Box-Behnken design. *Inorg Nano-Metal Chem* 49:33–43. doi:<https://doi.org/10.1080/24701556.2019.1583251>
53. Venil CK, Sathishkumar P, Malathi M, Usha R, Jayakumar R, Yusoff ARM, Ahmad WA (2016) Synthesis of flexirubin-mediated silver nanoparticles using *Chryseobacterium artocarpi* CECT 8497 and investigation of its anticancer activity. *Mater Sci Eng C* 59:228–234. <https://doi.org/10.1016/j.msec.2015.10.019>
54. Oun AA, Rhim JW (2017) Preparation of multifunctional chitin nanowhiskers/ZnO-Ag NPs and their effect on the properties of carboxymethyl cellulose-based nanocomposite film. *Carbohydr Polym* 169:467–479. doi:<https://doi.org/10.1016/j.carbpol.2017.04.042>
55. Shankar S, Rhim JW (2015) Amino acid mediated synthesis of silver nanoparticles and preparation of antimicrobial agar/silver nanoparticles composite films. *Carbohydr Polym* 130:353–363. doi:<https://doi.org/10.1016/j.carbpol.2015.05.018>
56. Taokaew S, Seetabhawang S, Siripong P, Phisalaphong M (2013) Biosynthesis and characterization of nanocellulose-gelatin films. *Materials* 6:782–794. <https://doi.org/10.3390/ma6030782>
57. Pereira R, Tojeira A, Vaz DC, Mendes A, Bártoło P (2011) Preparation and characterization of films based on alginate and aloe vera. *Int J Polym Anal Charact* 16:449–464. doi:<https://doi.org/10.1080/1023666X.2011.599923>
58. Singhal G, Bhavesh R, Kasariya K, Sharma AR, Singh RP (2011) Biosynthesis of silver nanoparticles using *Ocimum sanctum* (Tulsi) leaf extract and screening its antimicrobial activity. *J Nanoparticle Res* 13:2981–2988. <https://doi.org/10.1007/s11051-010-0193-y>
59. Sharma S, Kumar S, Bulchandani BD, Taneja S, Banyal S (2013) Green synthesis of silver nanoparticles and their antimicrobial activity against gram positive and gram negative bacteria. *Int J Biotechnol Bioeng Res* 4:711–714
60. Ibrahim HMM (2015) ScienceDirect Green synthesis and characterization of silver nanoparticles using banana peel extract and their antimicrobial activity against representative microorganisms. *J Radiat Res Appl Sci* 8:1–11. doi:<https://doi.org/10.1016/j.jrras.2015.01.007>
61. Kameswara Srikar S, Giri DD, Pal DB, Mishra PK, Upadhyay SN (2016) Green synthesis of silver nanoparticles: a review. *Green Sustain Chem* 6:34–56. <https://doi.org/10.4236/gsc.2016.61004>
62. Zhang S, Tang Y, Vlahovic BA (2016) Review on preparation and applications of silver-containing nanofibers. *Nanoscale Res Lett* 11:1–8. <https://doi.org/10.1186/s11671-016-1286-z>
63. Li MC, Wu Q, Song K, Cheng HN, Suzuki S, Lei T (2016) Chitin nanofibers as reinforcing and antimicrobial agents in carboxymethyl cellulose films: influence of partial deacetylation. *ACS Sustain Chem Eng* 4:4385–4395. <https://doi.org/10.1021/acsschemeng.6b00981>
64. Weerakkody NS, Caffin N, Turner MS, Dykes GA (2010) In vitro antimicrobial activity of less-utilized spice and herb extracts against selected food-borne bacteria. *Food Control* 21:1408–1414. doi:<https://doi.org/10.1016/j.foodcont.2010.04.014>
65. Hosseini MH, Razavi SH, Mousavi MA, Antimicrobial (2009) physical and mechanical properties of chitosan-based films incorporated with thyme, clove and cinnamon essential oils. *J Food Process Preserv* 33:727–743. doi:<https://doi.org/10.1111/j.1745-4549.2008.00307.x>

Publisher's Note Springer Nature remains neutral with regard to jurisdictional claims in published maps and institutional affiliations.